

In-plane Vibration Analysis of Symmetric Angle-ply Laminated Composite Arches

Mehmet ÇEVİK¹▲

¹*Dokuz Eylül University, İzmir Vocational School, 35150 Buca-Izmir, Turkey*

Received: 23.02.2009 Revised: 08.12.2009 Accepted: 25.12.2009

ABSTRACT

The in-plane free vibration analysis of symmetric angle-ply laminated composite arches is carried out by finite elements method. The rotary inertia and shear deformation effects have been included in the analysis. Arches with opening angle (α) from 30° to 270° are taken into consideration. Parametric studies are performed to study the effects of fiber orientation angle, boundary conditions, material orthotropy, radius-to-width ratio and number of layers on natural frequencies. The validity of the finite element model is shown by comparing the results with those available in the literature. Mode shapes are presented for two different cases. It is found that fundamental in-plane natural frequency of laminated composite arches can be substantially increased by 30 to 60%, by using angle-ply instead of cross-ply. This percent increase offers a considerable advantage that, for arch beams, angle-ply lamination can be preferable to cross-ply lamination.

Key Words: Arch, in-plane vibration, angle-ply laminated composite.

1. INTRODUCTION

In many engineering applications, arches have been widely used as structural elements; therefore, the vibrational behavior of arches has been of interest to many researchers [1-7]. Besides other materials, laminated composite materials have come into extensive use in the last decades. Studies on the vibrational analysis of laminated composite arches generally deal with out-of-plane vibrations. Khdeir and Reddy [8] developed a model for the dynamic behavior of a laminated composite shallow arch from shallow shell theory and determined exact natural frequencies of cross-ply laminated arches. Qatu and Elsharkawy [9] presented exact solutions for the vibration of laminated composite arches with deep curvature and arbitrary boundary

conditions and obtained natural frequencies using the Ritz method. Bhimaraddi [10] presented an accurate shear deformable theory for the analysis of the complete dynamic response of curved beams of constant curvature. Both in-plane and out-of-plane vibrations were analyzed and the effect of coupling was illustrated on various vibrational frequencies. Yıldırım [11] performed a numerical study to investigate the common effects of the rotary inertia and shear deformation on the out-of-plane free vibration frequencies of symmetric cross-ply laminated circular bars with the help of the transfer matrix method. Matsunaga [12] analyzed natural frequencies and buckling stresses of laminated composite circular arches subjected to initial axial stress.

▲Corresponding author, e-mail: mehmet.cevik@deu.edu.tr

Besides, there are few studies focusing on the in-plane vibrations of composite arches. Qatu [13] presented a complete set of equations for the free and forced in-plane vibration analysis of laminated composite beams of shallow curvature. Natural frequencies for simply supported curved beams were obtained by exact solutions. The Ritz method with algebraic polynomials was used to obtain approximate solutions for arbitrary boundary conditions. Yıldırım [14] studied the in-plane free vibrational analysis of symmetric cross-ply laminated circular arches using both the Timoshenko and Bernoulli-Euler beam theories, and the transfer matrix method. Radius/thickness ratios from 5 to 25, different boundary conditions, and two values of opening angles (10° and 90°) were considered in the parametric study. In another study [15], Yıldırım performed a parametric study to investigate influences of the opening angles, the slenderness ratios, the material types, the boundary conditions, and the thickness-to-width ratios of the cross section on the in-plane natural frequencies of symmetric cross-ply laminated circular composite beams. Tseng et al. [16] studied the free in-plane vibration of cross-ply laminated beams of variable curvature based on the Timoshenko-type curved beam theory. They developed an analytical solution by incorporating the dynamic stiffness method and the series solution. Ecsedi and Dluhi [17] presented a simple one-dimensional mechanical model to analyse the static and dynamic feature of non-homogeneous curved beams and closed rings. Natural frequencies for simply supported laminated composite curved beams were obtained by exact solution. Tanrıöver and Şenocak [18] considered large deflection analysis of composite plates. The Galerkin method along with the Newton-Raphson method is applied to large deflection analysis of laminated composite plates with various edge conditions. Yalcin et al. [19] proposed discrete and continuum models for layered composites based on a higher order dynamic approximate theory. Recently, Malekzadeh et al. [20] introduced an accurate and efficient solution procedure based on the two-dimensional elasticity theory for free vibration of arbitrary laminated thick circular deep arches with some combinations of classical boundary conditions. Lü and Lü [21] carried out exact analysis on the in-plane free vibration of simply supported laminated circular arches based on the two-dimensional theory of elasticity. Malekzadeh and Setoodeh [22] presented a differential quadrature solution, in which the governing equations are based on the Reissner-Naghdi type shell theory, for moderately thick laminated circular arches with general boundary conditions. Moleiro et al [23] developed new mixed least-squares finite element models for static and free vibration analysis of laminated composite plates. Jun et al. [24] used the dynamic stiffness method for studying the vibration characteristics of the laminated composite shallow circular arches.

In almost all of the research investigations on the vibrational analysis of laminated composite arches, cross-ply stacking sequences are considered. However, angle-ply stacking sequence can be favorable in certain opening angles of arches. In order to obtain any desired frequency in accordance with the opening angle of the arch,

different fiber angles should be used rather than cross-ply. The variation of the natural frequency of the arch with respect to the fiber angle, while opening angle changes, is not investigated thoroughly in the literature. In the present study, the in-plane free vibration analysis of symmetric angle-ply laminated composite arches is carried out by finite elements method using ANSYS 10.0 [25] commercial software. The rotary inertia and shear deformation effects have been included in the analysis. Arches with opening angle from 30° to 270° are taken into consideration. Parametric studies are performed to study the effects of especially fiber orientation angle, and also boundary conditions, material orthotropy, arch width and number of layers on natural frequencies.

2. FINITE ELEMENT MODELING OF THE LAMINATED COMPOSITE ARCH

The geometry of the laminated composite arch is illustrated in Figure 1. The radius, length, height (thickness) and width of the beam are represented by R , L , h and b , respectively. The length of the beam is $L = 2\pi R(\alpha/360)$ and it is taken at the center of b and h . Unless otherwise stated, $L/h = 15$ and $h = b = 1$. No dimensions are used for the sake of brevity. The composite arch beam has four layers $[\theta/-\theta/-\theta/\theta]$ of equal thickness. Lamination of the composite material model is shown in Figure 2.

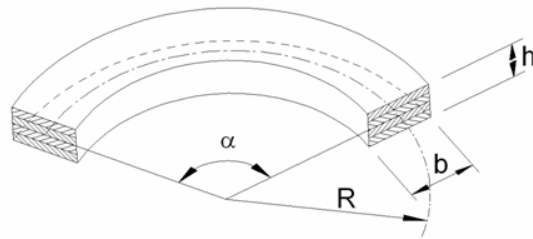


Figure 1. The geometry of the laminated composite arch.

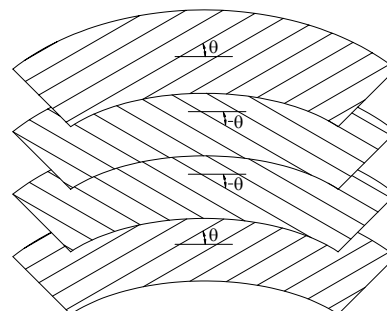


Figure 2. Lamination of the composite material model $[\theta/-\theta/-\theta/\theta]$.

In the present study, arches with opening angle (α) from 30° to 270° are considered. R/L ratios corresponding to the opening angles are shown in Table 1. In order to simulate the vibrations of the beam, the ANSYS 10.0

[25] finite element analysis software package is employed. 8-noded, linear layered 3-dimensional structural shell element (shell-99) having six degrees of freedom at each node (translations in the nodal x, y, and z directions and rotations about the nodal x, y, and z-axes) is used for modeling. Because of the finite element degrees of freedom, out-of-plane vibrations are also captured; however, these are investigated in an other study and are outside the scope of the present study. The

shell-99 element takes into consideration the rotary inertia and shear deformation effects. The arch is meshed into approximately 60 elements and 245 nodes based on a convergence study. Schematic finite element model of $\alpha=120^\circ$ arch in ANSYS is shown in Figure. 3. Note that the number of finite elements is altered appropriately where necessary. Since in-plane bending and axial vibrations are always coupled in angle-ply stacking sequences, this is also taken into account in the analysis.

Table 1. *R/L* ratios corresponding to the opening angles.

Opening angle (°)	30	60	90	120	150	180	210	240	270
<i>R/L</i>	1.91	0.95	0.64	0.48	0.38	0.32	0.27	0.24	0.21

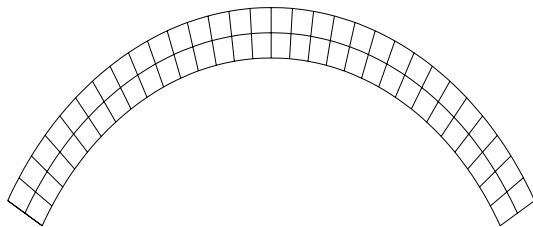


Figure 3. Schematic finite element model of $\alpha = 120^\circ$ arch in ANSYS. ($L/h = 15, h/b = 1$).

3. VERIFICATION OF THE FINITE ELEMENT MODEL

In order to validate the accuracy and applicability of the present model, numerical results are compared with those available in the literature. For this purpose, two examples are considered. In the first example, the in-plane vibration problem of a symmetric $[0^\circ/90^\circ/90^\circ/0^\circ]$ graphite-epoxy straight beam ($L/h=10, h/b=1$) is handled. The material properties are as follows: $E_1 = 144.8$ GPa, $E_2 = 9.65$ GPa, $G_{12} = G_{13} = 4.14$ GPa, $G_{23} = 3.45$ GPa, $\nu_{12} = 0.3, \rho = 1389.23$ Ns²/m⁴ where E, G and ν are the modulus of elasticity, shear modulus and Poisson's ratio, respectively. The first six dimensionless in-plane natural frequencies $[\Omega = \omega L^2(\rho/E_1 h^2)^{1/2}]$ of the beam are compared with the results of Yıldırım [14] for clamped-clamped (C-C) and clamped-free (C-F) boundary conditions in Table 2. As seen from the table, the present model yielded results in good agreement with those of Ref. [14].

Table 2. Comparison of the first six dimensionless in-plane natural frequencies of a $[0^\circ/90^\circ/90^\circ/0^\circ]$ graphite-epoxy straight beam ($L/h=10, h/b=1$).

Modes	Yıldırım [14]		Present study	
	C-C	C-F	C-C	C-F
1	3.3874	0.7098	3.4098	0.7115
2	7.4350	3.6369	7.5231	3.6557
3	12.1429	8.3354	12.3358	8.4062
4	17.0922	11.4715	17.4248	11.4982
5	22.1391	13.4299	22.6493	13.5907
6	22.9428	18.6600	22.9958	18.9536

As a second example, fundamental in-plane dimensionless natural frequencies $[\Omega = \omega L^2(\rho/E_2 h^2)^{1/2}]$ of $[0^\circ/90^\circ/0^\circ]$ beam with varying opening angle (α) and varying E_1/E_2 ratio are considered. The beam has clamped-clamped boundary conditions and $L/h=10, h/b=1$. Table 3 shows a comparison of the results of Ref. [14] with the present frequencies. Considering Table 3, the author thinks that the results of Ref. [14] are incorrect for $\alpha=10^\circ$. The dimensionless frequencies of a shallow arch ($\alpha=10^\circ$) must be close to those of a straight beam. However, for $\alpha=10^\circ$, the frequency values of [14] are extremely high. On the other hand, the frequencies of $\alpha=90^\circ$ arch of [14] are, unexpectedly, very close to those of the straight beam.

Table 3. Comparison of the dimensionless fundamental in-plane natural frequencies of [0°/90°/0°] beam for C-C boundary conditions ($L/h=10, h/b=1$).

	E_1/E_2	Ref. [14]	Present
straight beam	1	-	6.1983
	20	-	16.4156
	40	-	18.7998
$\alpha=10^\circ$	1	108.31	6.3605
	20	129.89	17.3274
	40	134.72	20.3944
$\alpha=90^\circ$	1	6.217	13.8511
	20	16.759	31.7100
	40	19.273	34.6464

Considering the two examples, it has been concluded that the results of the present study are acceptable and can be used in the parametric study.

4. NUMERICAL RESULTS AND DISCUSSION

In this section, the effects of different parameters on the dimensionless in-plane natural frequency (Ω) of symmetric angle-ply arches are considered. The orthotropic material properties of the composite layers are: $E_1/E_2 = 40, G_{12} = G_{13} = 0.6E_2, G_{23} = 0.5E_2, \nu_{12} = 0.25$.

Variations of the fundamental Ω of symmetric [0°/-θ°/-θ°/0°] angle-ply arches are presented in Figures 4-8 with varying fiber angle (θ) and opening angle (α) for various boundary conditions.

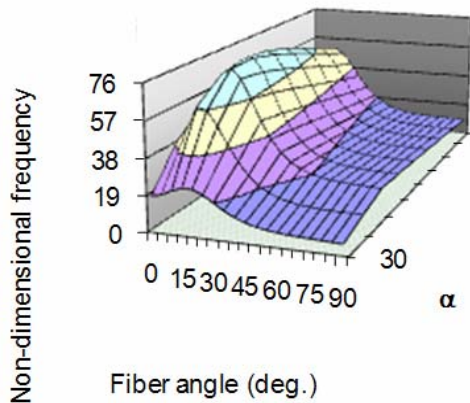


Figure 4. Fundamental Ω of [0°/-θ°/-θ°/0°] angle-ply arch as a function of fiber angle and opening angle (α) for C-C boundary conditions.

Figure 4 shows the variation of fundamental Ω for clamped-clamped boundary conditions. The frequency takes its lowest values at $\alpha=30^\circ$. As the opening angle increases, the frequency increases rapidly and reaches its maximum value at about $\alpha=90^\circ$. After these values, the frequency begins to decrease up to $\alpha=270^\circ$ of opening angle. On the other hand, for any value of opening angle, fundamental Ω increases up to about 10°-15° fiber angle, reaches its maximum and then decreases gradually up to 90° fiber angle. For $\alpha=90^\circ$, the maximum frequency is 72.5384 with $\theta = 15^\circ$. For $\theta \geq 15^\circ$, the maximum frequency occurs at $\alpha=90^\circ$. For $\theta = 10^\circ$, the maximum frequency occurs at $\alpha=120^\circ$ while for $\theta \leq 5^\circ$ it occurs at $\alpha=150^\circ$.

Figure 5 - 6 show the variation of fundamental Ω for clamped-hinged (C-H) and hinged-hinged (H-H) end conditions, respectively. The variations are similar to that of clamped-clamped case. In C-H case, the maximum Ω is 61.0645 for $\alpha=90^\circ$ with $\theta = 15^\circ$, and in H-H case the maximum Ω is 50.6375 for $\alpha=90^\circ$ with

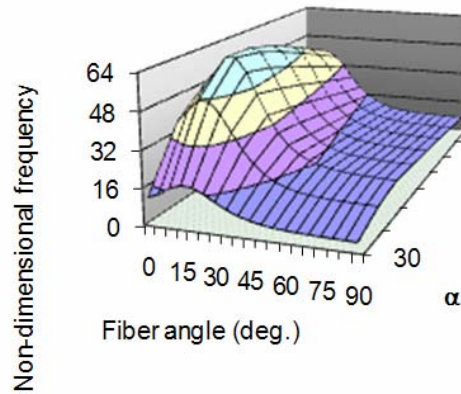


Figure 5. Fundamental Ω of [0°/-θ°/-θ°/0°] angle-ply arch as a function of fiber angle and opening angle (α) for C-H boundary conditions.

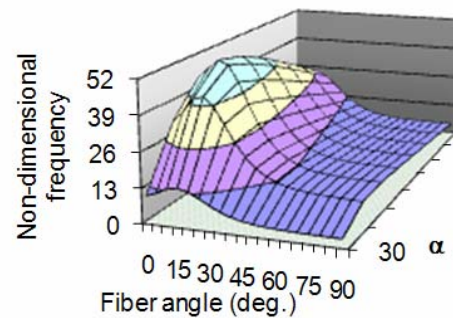


Figure 6. Fundamental Ω of [0°/-θ°/-θ°/0°] angle-ply arch as a function of fiber angle and opening angle (α) for H-H boundary conditions.

Figure 7 shows the variation of fundamental Ω for C-F end conditions. In this case, increasing opening angle always results in an increase in frequency. For opening angles $\alpha \leq 120^\circ$, the maximum frequency occurs at about 5° - 10° fiber angle. For $\alpha \geq 150^\circ$, the maximum frequency is at $\theta = 0^\circ$ and increasing fiber angle decreases Ω . Considering C-F end conditions, the maximum dimensionless frequency is 8.8925 at $\alpha = 240^\circ$ and $\theta = 0^\circ$.

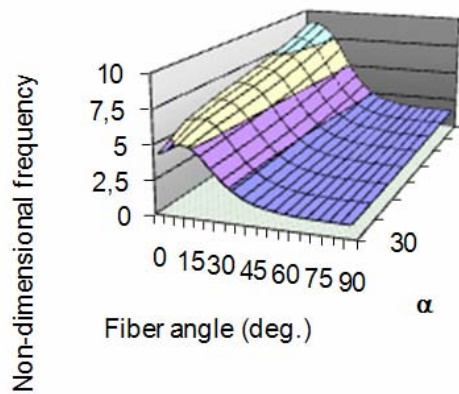


Figure 7. Fundamental Ω of $[\theta/-\theta/-\theta/\theta]$ angle-ply arch as a function of fiber angle and opening angle (α) for C-F boundary conditions.

Figure 8 shows the variation of Ω for free-free (F-F) end conditions. The variation in this case is also similar to that of C-C case. For any value of opening angle, the maximum frequency occurs at 5° - 10° fiber angle. The maximum value of Ω is 33.4968 at $\alpha = 90^\circ$ and $\theta = 10^\circ$.

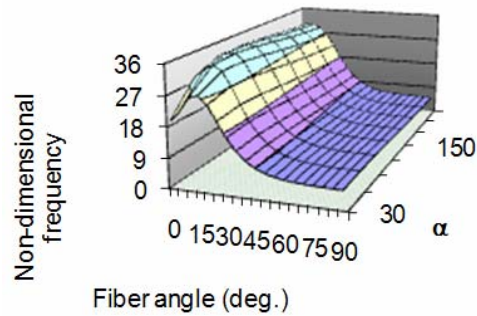


Figure 8. Fundamental Ω of $[\theta/-\theta/-\theta/\theta]$ angle-ply arch as a function of fiber angle and opening angle (α) for Free-Free boundary conditions.

In Figures 9-12, variations of the lowest six Ω are shown for C-C arches of four different opening angles (30° , 90° , 180° and 270°). In all cases, the frequency increases up to about 10° - 20° fiber angle, and then decreases gradually up to 90° . The mode shapes change from flexural into axial (or from axial into flexural) where the frequency curves approach each other. (Examples: For $\alpha = 30^\circ$, 5th and 6th modes at $\theta = 10^\circ$, 4th and 5th modes at $\theta = 25^\circ$; for $\alpha = 90^\circ$, 3rd and 4th modes at $\theta = 5^\circ$, 5th and 6th modes at $\theta = 15^\circ$) It is observed that this curve veering is more frequent at $\alpha = 30^\circ$ and becomes rare as the opening angle increases.

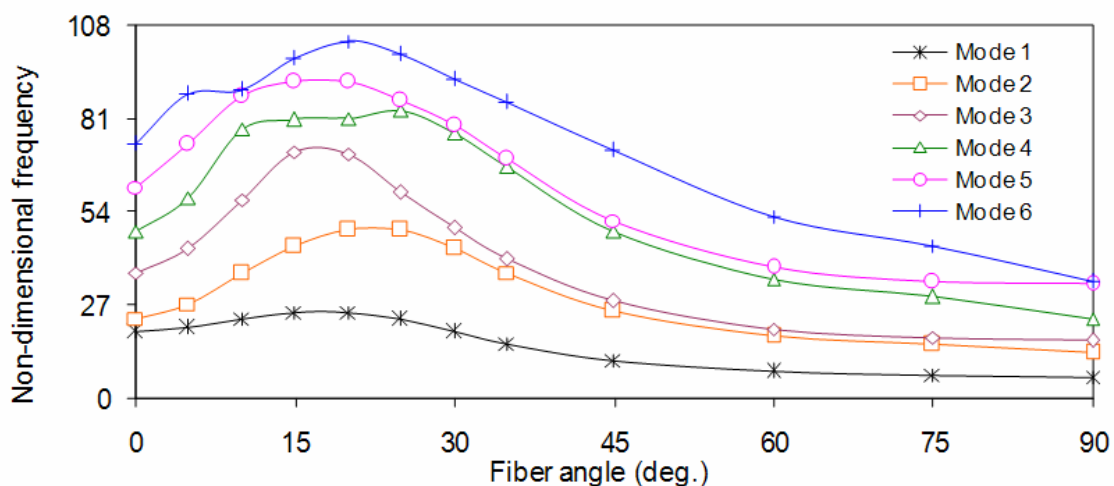


Figure 9. Variation of the lowest six Ω with fiber angle for the C-C arch of $\alpha = 30^\circ$.

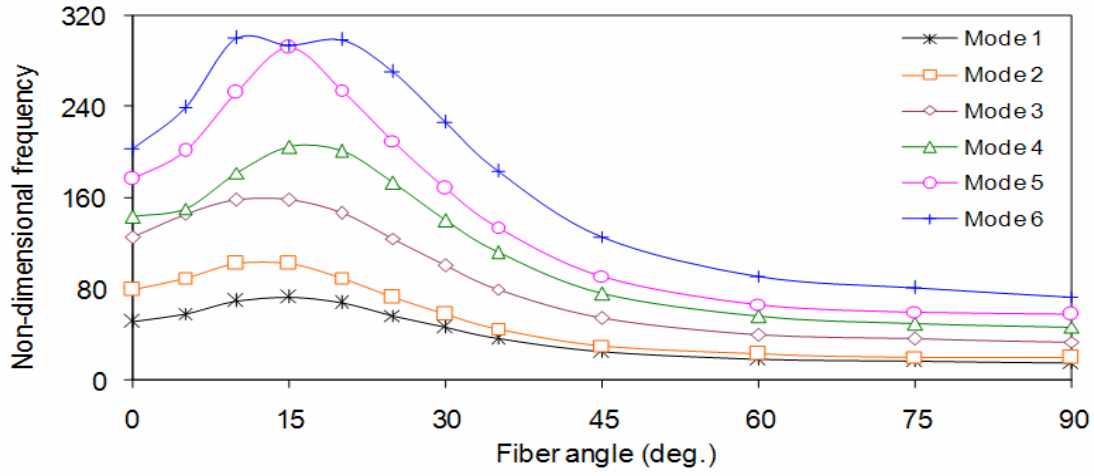


Figure 10. Variation of the lowest six Ω with fiber angle for the C-C arch of $\alpha=90^\circ$.

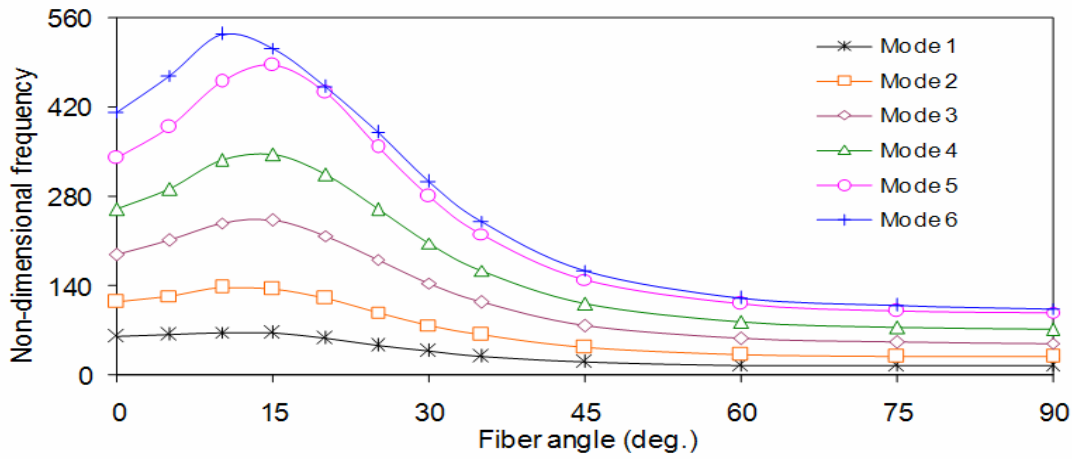


Figure 11. Variation of the lowest six Ω with fiber angle for the C-C arch of $\alpha=180^\circ$.

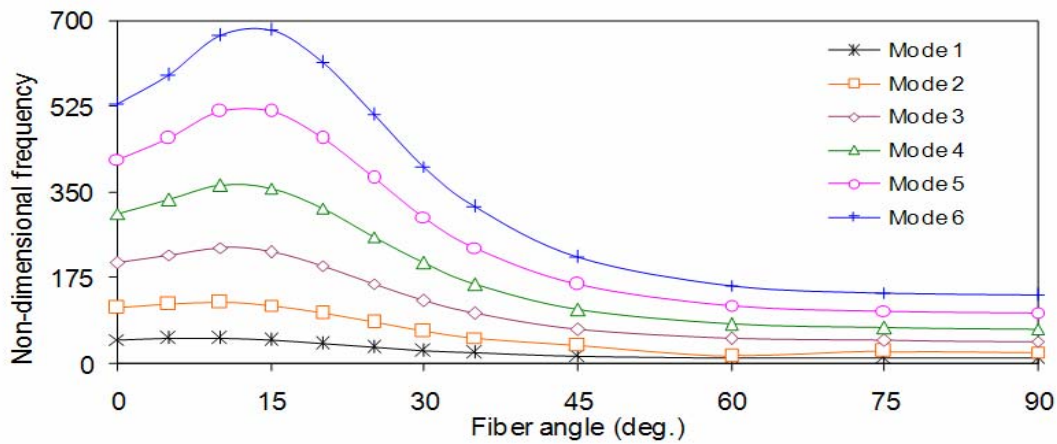


Figure 12. Variation of the lowest six Ω with fiber angle for the C-C arch of $\alpha=270^\circ$.

Figure 13 shows the effect of the width of the arch on the fundamental dimensionless frequency for C-C boundary conditions. It is observed that increasing the width of the beam will result in a proportional increase in the dimensionless fundamental frequency. It is ascertained here that the maximum Ω occurs at about 15° fiber angle.

Figure 14 shows the effect of the ratio of the extensional modulus to the transverse modulus on the fundamental Ω for C-C boundary conditions. It is clear that increasing the modulus ratio will increase the frequency up to a fiber angle of $\theta = 60^\circ$. Above this value, the modulus ratio has no effect.

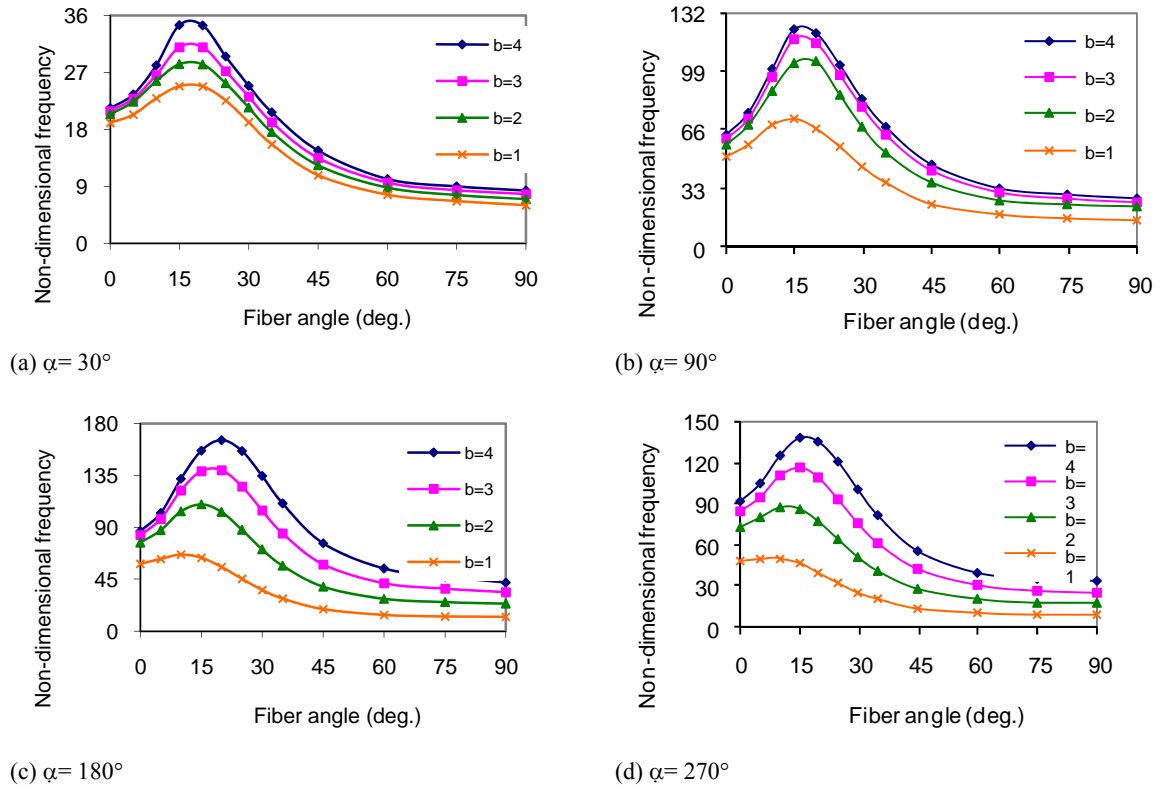
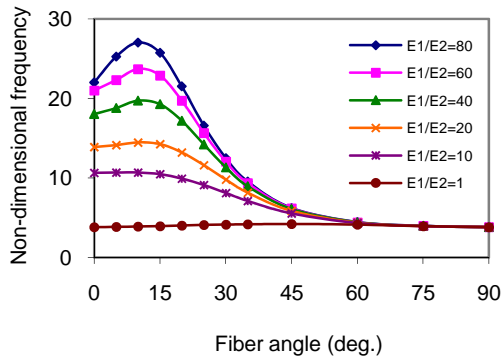
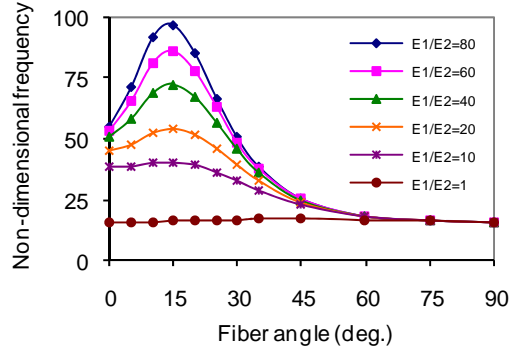


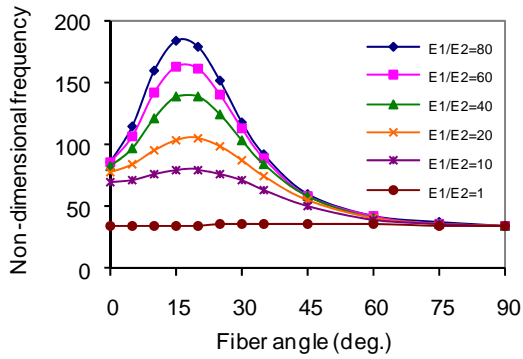
Figure 13. Effect of the width of the arch beam on the fundamental Ω .



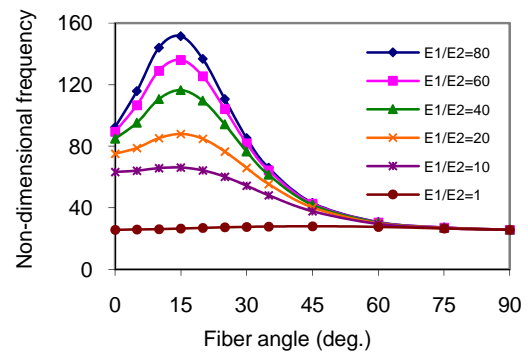
(a) $\alpha=30^\circ$



(b) $\alpha=90^\circ$



(c) $\alpha=180^\circ$



(d) $\alpha=270^\circ$

Figure 14. Effect of the modulus ratio on the fundamental Ω .

Table 4 shows the effect of layer number on the fundamental Ω for C-C boundary conditions. It can be seen that the frequency increases with increasing number of layers from 2 to 4 for angle-ply lamination.

On the other hand, the maximum frequency occurs at 3 layers for cross-ply lamination. Balanced stacking sequences result in the same frequency not depending on the number of layers, as expected.

Table 4. Effect of layer number on the fundamental dimensionless frequency for C-C boundary conditions.

Opening angle (α)	Stacking sequence	Fiber angle (θ)				cross-ply
		0°	30°	45°	60°	
30°	[θ /- θ]	19.0327	15.7542	9.9367	7.3905	13.2614
	[θ /- θ / θ]	19.0327	18.7373	10.6890	7.6300	16.8257
	[θ /- θ /- θ / θ]	19.0327	19.1243	10.7621	7.6508	15.5081
	[θ /- θ / θ /- θ] _s	19.0327	19.1243	10.7621	7.6508	15.5081
90°	[θ /- θ]	51.0257	37.6003	23.1834	17.6257	42.5364
	[θ /- θ / θ]	51.0257	44.9005	24.5866	17.9370	48.1659
	[θ /- θ /- θ / θ]	51.0257	45.6250	24.6934	17.9606	45.7151
	[θ /- θ / θ /- θ] _s	51.0257	45.6250	24.6934	17.9606	45.7151
180°	[θ /- θ]	58.4786	29.3440	18.0656	13.8163	45.4934
	[θ /- θ / θ]	58.4786	35.1745	19.0737	13.9960	52.3763
	[θ /- θ /- θ / θ]	58.4786	35.6820	19.1444	14.0085	47.6758
	[θ /- θ / θ /- θ] _s	58.4786	35.6820	19.1444	14.0085	47.6758

4.1. Comparison with Cross-ply Lamination

In order to make a comparison between cross-ply and angle-ply laminations, fundamental Ω of symmetric cross-ply and maximum fundamental Ω of symmetric [θ /- θ /- θ / θ] angle-ply laminated composite arches are tabulated in Table 5-6 for different opening angles and boundary conditions. Evaluating Table 5 and Figure

4-8 together, it is seen that, for arches of opening angle $\alpha=30^\circ$, the natural frequencies of cross-ply lamination correspond to those of angle-ply lamination with fiber angle around 30° . In arches of opening angle $\alpha \geq 60^\circ$, the natural frequencies of cross-ply lamination correspond to those of angle-ply lamination with fiber angle about 20° - 25° .

Table 5. Fundamental Ω of symmetric cross-ply laminated composite arches.

Opening angle (°)	Boundary condition				
	C-C	C-H	H-H	C-F	F-F
30	15.5080	11.7173	9.9606	3.6701	18.0373
60	37.0337	33.5812	28.6835	4.3925	23.7504
90	45.7152	42.2800	36.4633	4.6870	24.8962
120	49.3471	43.1310	35.1135	4.9385	24.6199
150	49.5506	41.1734	31.7534	5.2247	23.9212
180	47.6758	37.7716	27.4513	5.5719	23.1724
210	44.6529	33.7105	22.7813	5.9968	22.5265
240	41.1066	29.4520	18.0104	6.5182	22.0666

Table 6. Maximum fundamental Ω of symmetric $[\theta/-\theta/-\theta/\theta]$ angle-ply laminated composite arches.

Opening angle (°)	Boundary condition				
	C-C	C-H	H-H	C-F	F-F
30	24.8323	19.0353	14.4908	5.2054	27.8812
60	58.0742	47.4423	41.8821	5.8914	32.8679
90	72.5384	61.0645	50.6375	6.3214	33.4968
120	72.3605	60.3386	47.8434	6.6783	33.0608
150	70.2606	56.6221	42.7882	7.0943	32.2291
180	66.3571	51.3502	36.7469	7.5859	31.2782
210	61.2987	45.4664	30.5588	8.1744	30.4399
240	55.8325	39.4895	24.2185	8.8925	29.876

Figure. 15 illustrates the percent difference between the fundamental Ω of cross-ply lamination and maximum fundamental Ω of angle-ply lamination, for comparison purposes. It is clear, from the figure, that the fundamental in-plane Ω of laminated composite arches can be increased by at least 34% up to a maximum of about 62%, by means of using angle-ply lamination instead of cross-ply. This percent increase represents a considerable advantage which should not be disregarded in design. The difference is higher at lower opening angles; and C-C boundary condition

offers the greatest advantage.

4.2. Mode Shapes

Figure 16 shows mode shapes of the lowest six in-plane modes of the C-C arch of $\alpha=90^\circ$ opening angle with stacking sequence $[30^\circ/-30^\circ/-30^\circ/30^\circ]$. Coupling between in-plane bending and axial vibrations is obvious in fourth and fifth modes. Also shown in Figure 17 are the mode shapes of the lowest six in-plane modes of the C-F arch of $\alpha=180^\circ$ opening angle with stacking sequence $[45^\circ/-45^\circ/-45^\circ/45^\circ]$.

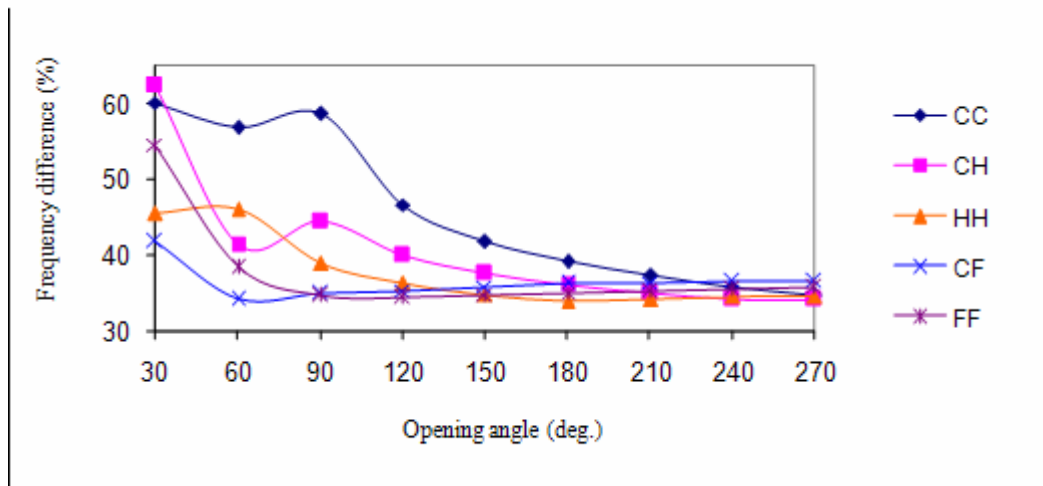


Figure 15. Percent difference between the frequencies of cross-ply lamination and maximum frequencies of angle-ply lamination.

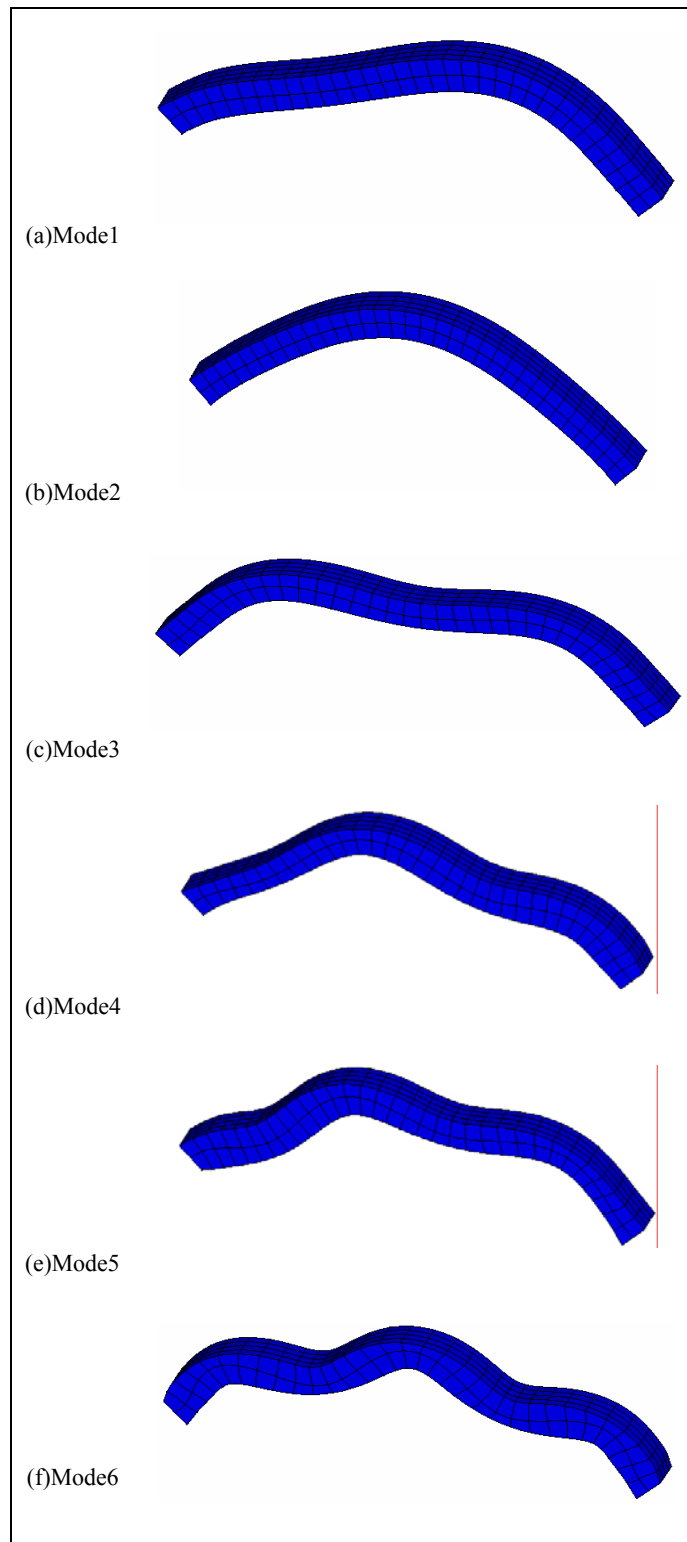


Figure 16. Mode shapes of the lowest six in-plane modes of the C-C arch of $\alpha=90^\circ$ opening angle with stacking sequence $[30^\circ/-30^\circ/-30^\circ/30^\circ]$.

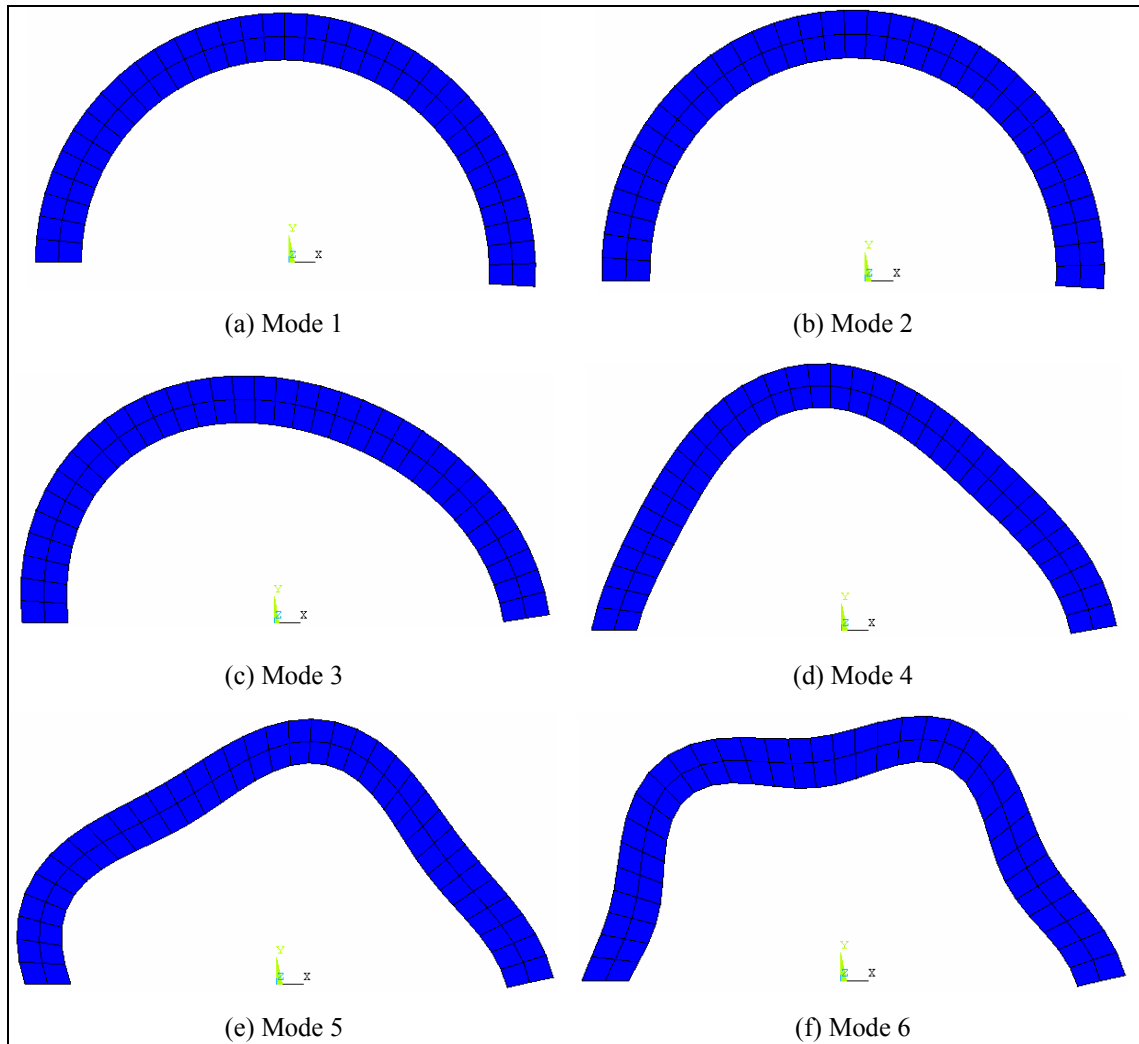


Figure 17. Mode shapes of the lowest six in-plane modes of the C-F arch of $\alpha=180^\circ$ opening angle with stacking sequence $[45^\circ/-45^\circ/-45^\circ/45^\circ]$.

5. CONCLUSIONS

The in-plane free vibration analysis of symmetric angle-ply laminated composite arches is carried out by finite elements method. Under any boundary conditions except for C-F, the frequencies take their lowest values at $\alpha=30^\circ$. As the opening angle increases, the frequencies increase rapidly and reach their maximum values at about $\alpha=90^\circ$. After these values, the frequencies begin to decrease up to $\alpha=270^\circ$ of opening angle. On the other hand, for any value of opening angle, fundamental in-plane frequency increases up to about 10° - 15° fiber angle, reaches its maximum and then decreases gradually up to 90° fiber angle. Under C-F boundary conditions, increasing opening angle always results in an increase in frequency. Considering higher modes of C-C boundary conditions, the frequency increases up to about 10° - 20° fiber angle, and then decreases gradually up to 90° in all modes. The change of mode shapes from flexural into axial is more frequent in lower opening angles and becomes rare as the opening angle increases. Increasing the modulus ratio will increase the frequency up to a fiber angle of θ

$=60^\circ$. Above this value, the modulus ratio has no effect. The frequency increases with increasing number of layers from 2 to 4 for angle-ply lamination.

The most significant finding of the present study is that the fundamental in-plane natural frequency of laminated composite arches can be increased by at least 34% up to a maximum of about 62%, by means of using angle-ply lamination instead of cross-ply. This percent increase represents a considerable advantage which should not be disregarded in design.

ACKNOWLEDGEMENT

This study was partly supported by the Scientific and Technological Research Council of Turkey (TUBITAK) under project number 106M154.

REFERENCES

- [1] Chidamparam, P. and Leissa, A.W., "Vibrations of Planar Curved Beams, Rings, and Arches", *Appl. Mechanics Review*, 46(3-5): 467-483 (1993).

- [2] Howson, W.P. and Jemah, A.K., "Exact Out-of-Plane Natural Frequencies of Curved Timoshenko Beams", *ASCE J. of Eng. Mechanics*, 125(1): 19-25 (1999).
- [3] Eisenberger, M. and Efraim, E., "In-Plane Vibrations of Shear Deformable Curved Beams", *Int. J. for Numerical Methods in Eng.*, 52(11): 1221-1234 (2001).
- [4] Wu, J.-S. and Chiang, L.-K., "Free Vibration Analysis of Arches Using Curved Beam Elements", *Int. J. for Numerical Methods in Eng.*, 58(13): 1907-1936 (2003).
- [5] Karami, G. and Malekzadeh, P., "In-Plane Free Vibration Analysis of Circular Arches with Varying Cross Sections Using Differential Quadrature Method", *J. Sound and Vibration*, 274(3-5): 777-799 (2004).
- [6] Chen, C.-N., "DQEM Analysis of In-Plane Vibration of Curved Beam Structures", *Advances in Engineering Software*, 36(6): 412-424 (2005).
- [7] Oz, H.R. and Daş, M.T., "In-Plane Vibrations of Circular Curved Beams with a Transverse Open Crack", *Math. and Computational Applications*, 11(1): 1-10 (2006).
- [8] Khdeir, A.A. and Reddy, J.N., "Free and Forced Vibration of Cross-ply Laminated Composite Shallow Arches", *Int. J. of Solids & Structures*, 34(10): 1217-1234 (1997).
- [9] Qatu, M.S., Elsharkawy, A., "Vibration of Laminated Composite Arches with Deep Curvature and Arbitrary Boundaries", *Computers & Structures*, 47(2): 305-311 (1993).
- [10] Bhimaraddi, A., "Generalized Analysis of Shear Deformable Rings and Curved Beams", *Int. J. of Solids & Structures*, 24(4): 363-373 (1988).
- [11] Yıldırım, V., "Common Effects of the Rotary Inertia and Shear Deformation on the Out-of-plane Natural Frequencies of Composite Circular Bars", *Composites Part B: Engineering*, 32(8):687-695 (2001).
- [12] Matsunaga, H., "Free Vibration and Stability of Laminated Composite Circular Arches Subjected to Initial Axial Stress", *J. Sound and Vibration*, 271(3-5):651-670 (2004).
- [13] Qatu, M.S., "In-Plane Vibration of Slightly Curved Laminated Composite Beams", *J. Sound and Vibration*, 159(2): 327-338 (1992).
- [14] Yıldırım, V., "Rotary Inertia, Axial and Shear Deformation Effects on the In-Plane Natural Frequencies of Symmetric Cross-ply Laminated Circular Arches", *J. Sound and Vibration*, 224(4): 575-589 (1999).
- [15] Yıldırım, V., "In-Plane Free Vibration of Symmetric Cross-ply Laminated Circular Bars", *ASCE J. of Eng. Mechanics*, 125(6): 630-636 (1999).
- [16] Tseng, Y.P., Huang, C.S. and Kao, M.S., "In-Plane Vibration of Laminated Curved Beams with Variable Curvature by Dynamic Stiffness Analysis", *Composite Structures*, 50(2): 103-114 (2000).
- [17] Ecsedi, I. and Dluhi, K., "A Linear Model for the Static and Dynamic Analysis of Non-homogeneous Curved Beams", *Appl. Math. Modeling*, 29(12):1211-1231 (2005).
- [18] Tanrıöver, H. and Şenocak, E., "Large Deflection Analysis of Unsymmetrically Laminated Composite Plates: Analytical-numerical Type Approach", *Non-Linear Mechanics*, 39(8):1385-1392 (2004).
- [19] Yalçın, O.F., Mengi, Y. and Turhan, D., "Higher Order Approximate Dynamic Models for Layered Composites", *Eur. J. of Mechanics A/Solids*, 26(3): 418-441 (2007).
- [20] Malekzadeh, P., Setoodeh, A.R. and Barmshouri, E., "A Hybrid Layerwise and Differential Quadrature Method for In-plane Free Vibration of Laminated Thick Circular Arches", *J. Sound and Vibration*, 315(1-2): 212-225 (2008).
- [21] Lü, Q. and Lü, C.F., "Exact Two-dimensional Solutions for In-plane Natural Frequencies of Laminated Circular Arches", *J. Sound and Vibration*, 318(4-5): 982-990 (2008).
- [22] Malekzadeh, P. and Setoodeh, A.R., "DQM In-plane Free Vibration of Laminated Moderately Thick Circular Deep Arches", *Advances in Eng. Software*, 40(9): 798-803 (2009).
- [23] Moleiro, F., Mota Soares, C.M., Mota Soares, C.A. and Reddy, J.N., "Mixed Least-Squares Finite Element Models for Static and Free Vibration Analysis of Laminated Composite Plates", *Comp. Meth. In Appl. Mech. And Eng.*, 198 (21-26): 1848-1856 (2009).
- [24] Jun, L., Hongxing, H. and Rongying, S., "Free Vibration of Laminated Composite Circular Arches by Dynamic Stiffness Analysis", *J. Reinforced Plastics and Composites*, 27(8):851-870 (2008).
- [25] ANSYS 10.0 User's Manual (2005).